Supplementary information for

Strain-phonon coupling in (111)-oriented perovskite oxides

Magnus Moreau,[1] Astrid Marthinsen,[2] Sverre M. Selbach,[2] and Thomas Tybell[1,]*

1) Department of Electronic Systems, NTNU Norwegian University of Science and Technology, 7491 Trondheim, Norway

2) Department of Materials Science and Engineering, NTNU Norwegian University of Science and Technology, 7491 Trondheim, Norway

*E-mail: thomas.tybell@iet.ntnu.no

OCTAHEDRAL DISTORTIONS

Imposing strain will result in a distorted unit cell, affecting the oxygen octahedra structure. In order to establish an overall non-material specific picture, the response of $P4/mmm$ ((001)-strain) and $R\bar{3}m$ ((111)-strain) to strain structures is presented. For the $P4/mmm$ structure under (001)-strain the octahedra are tetragonally distorted, giving different BO bond lengths for the in- and out-of-plane directions. The tetragonality, defined c/a, depends on both in-plane strain $\epsilon_{(001)}$ and the Poisson's ratio $\nu_{(001)}$. Relying on

$$a = a_0(1 + \epsilon_{(001)}), \quad \text{(S1)}$$

$$c = a_0(1 + \epsilon_{(001),\perp}), \quad \text{(S2)}$$

$$\frac{\epsilon_\perp}{\epsilon} = \frac{-2\nu}{1-\nu}, \quad \text{(S3)}$$

where $\epsilon_{(001)}$, $\epsilon_{(001),\perp}$ and are the in-plane and out-of-plane strain in the (001)-plane respectively, a_0 is the lattice parameter of the aristotype $Pm\bar{3}m$ structure, and ν is the Poisson's ratio corresponding to the strain plane, the following expression for the degree of tetragonality under (001)-strain is obtained:

$$\frac{c}{a} = \frac{2\epsilon_{(001)}\nu_{(001)} + \nu_{(001)} - 1}{(1+\epsilon_{(001)})(\nu_{(001)} - 1)} \quad . \tag{S4}$$

For the $R\bar{3}m$ structure under (111)-strain all B-O bond lengths are equal. However, the rhombohedral has a pseudocubic cell angle α_{pc} that will deviate from the aristotype value of 90° as shown in Figure S1 a). As a consequence, the oxygen octahedra are distorted with O-B-O angles equal to α_{pc}. Based on this α_{pc} is used as a measure of octahedral distortion under (111)-strain. Using the identities

$$a_H^2 = 2a_0^2\left(1 - \cos\alpha_{pc}\right), \tag{S5}$$

$$c_H^2 = 3a_0^2(1 + 2\cos\alpha_{pc}), \tag{S6}$$

where a_H and c_H are the lattice parameters of the of the $R\bar{3}m$ structure in the hexagonal setting given by

$$a_H = \sqrt{2}a_0(1 + \epsilon_{(111)}), \tag{S7}$$

$$c_H = \sqrt{3}a_0\left(1 + \epsilon_{(111),\perp}\right), \tag{S8}$$

where $\epsilon_{(111)}$, and $\epsilon_{(111),\perp}$ are the in-plane and out-of-plane strain in the (111)-plane respectively, the following relationship between pseudocubic cell angle α_{pc}, the in-plane strain, $\epsilon_{(111)}$, and the Poisson's ratio, $\nu_{(111)}$ is obtained:

$$\cos\alpha_{pc} = \frac{\left(\frac{1-\frac{2\,\nu_{(111)}}{1-\nu_{(111)}}\epsilon_{(111)}}{1+\epsilon_{(111)}}\right)^2 - 1}{\left(\frac{1-\frac{2\,\nu_{(111)}}{1-\nu_{(111)}}\epsilon_{(111)}}{1+\epsilon_{(111)}}\right)^2 + 2}. \tag{S9}$$

The dependence of α_{pc} on strain, $\epsilon_{(111)}$, and Poisson's ratio, $\nu_{(111)}$, is plotted as a contour plot in Figure S1 b). The amount of octahedral distortions increases non-linearly with both increasing strain and Poisson's ratio. As the angle is no longer, 90 degrees, it will remove the three mirror planes and affect the strain response.

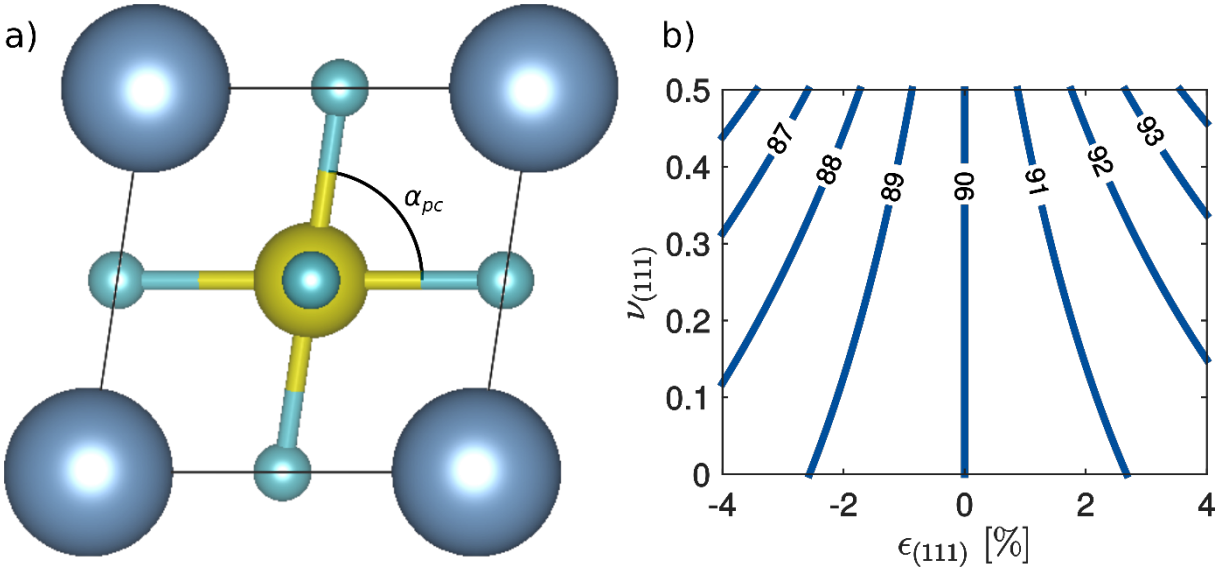

Figure S1: a) Illustration of the pseudocubic cell angle α_{pc} in the $R\bar{3}m$ structure. b) Contour plot of α_{pc} given in degrees as a function of strain in the (111)-plane, $\epsilon_{(111)}$, and the Poisson's ratio for (111)-strain, $\nu_{(111)}$.

DATA FOR COMPLEMENTING MATERIALS

In the main text we showed how the different phonon modes depends on strain in $SrTiO_3$ and $NaTaO_3$, here we show the same information for the 18 other materials studied in this work. First we present the results for III-III, then II-IV and finally I-V perovskites.

- Figures S2-S9 shows the strain phonon coupling for $LaAlO_3$, $NdAlO_3$, $LaGaO_3$, $LaFeO_3$, $NdGaO_3$, $YAlO_3$, $GdScO_3$ and $DyScO_3$ respectively.
- Figures S10-S14 shows the strain phonon coupling for $BaTiO_3$, $BaZrO_3$, $CaTiO_3$, $SrZrO_3$ and $MgTiO_3$ respectively.
- Figures S15-S19 shows the strain phonon coupling for $KNbO_3$, $KTaO_3$, $AgNbO_3$, $NaNbO_3$ and $LiNbO_3$ respectively.

III-III Perovskites

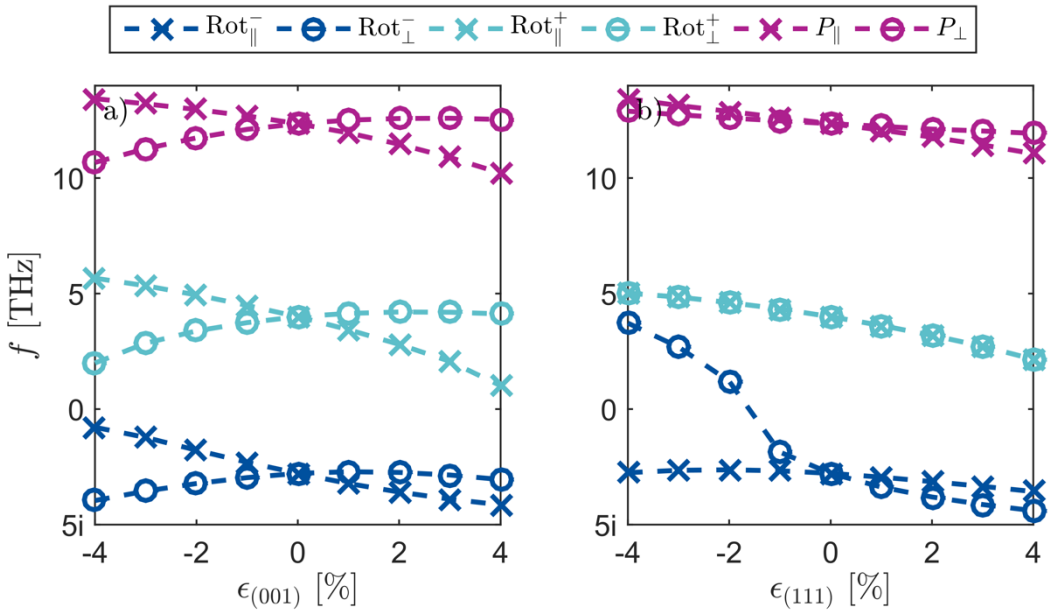

Figure S2: the frequencies of the three different phonon modes considered as a function of in-plane strain in the a) (001)-plane and b) (111)-plane for $LaAlO_3$.

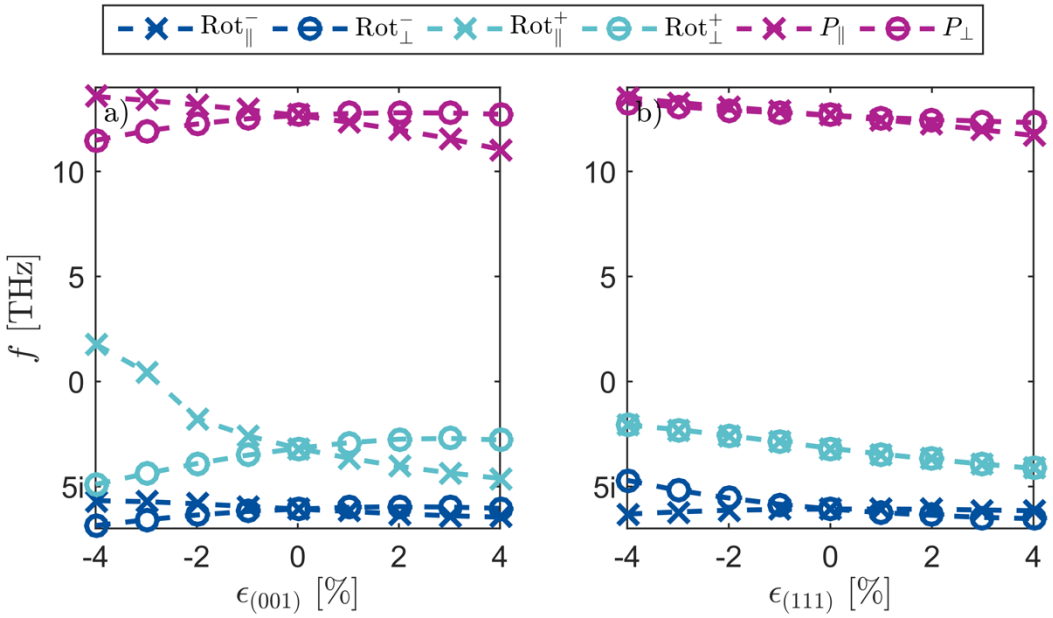

Figure S3: the frequencies of the three different phonon modes considered as a function of in-plane strain in the a) (001)-plane and b) (111)-plane for $NdAlO_3$.

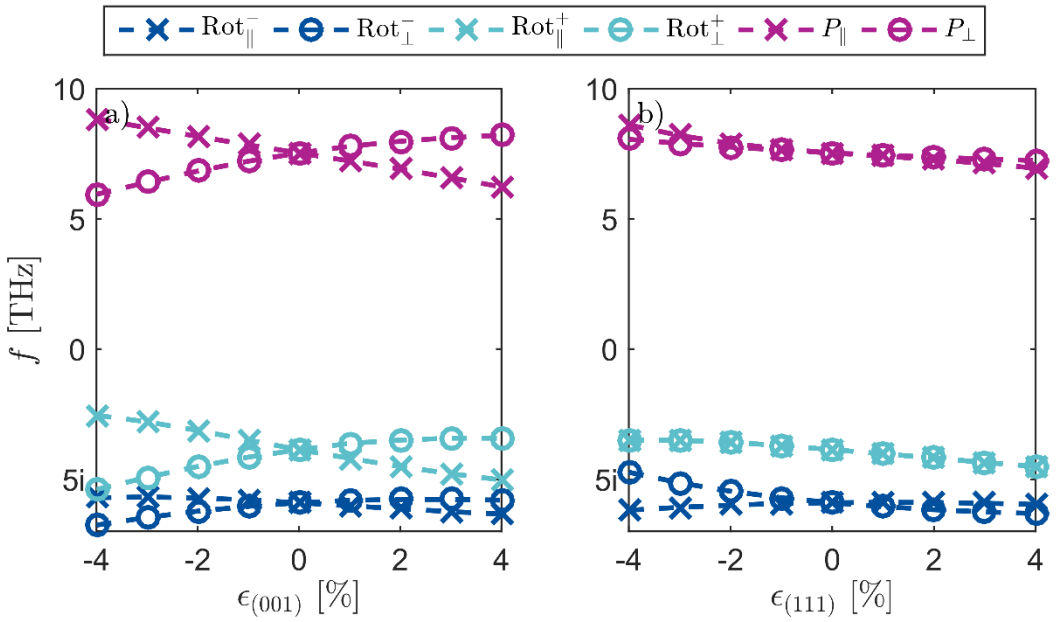

Figure S4: the frequencies of the three different phonon modes considered as a function of in-plane strain in the a) (001)-plane and b) (111)-plane for $LaGaO_3$.

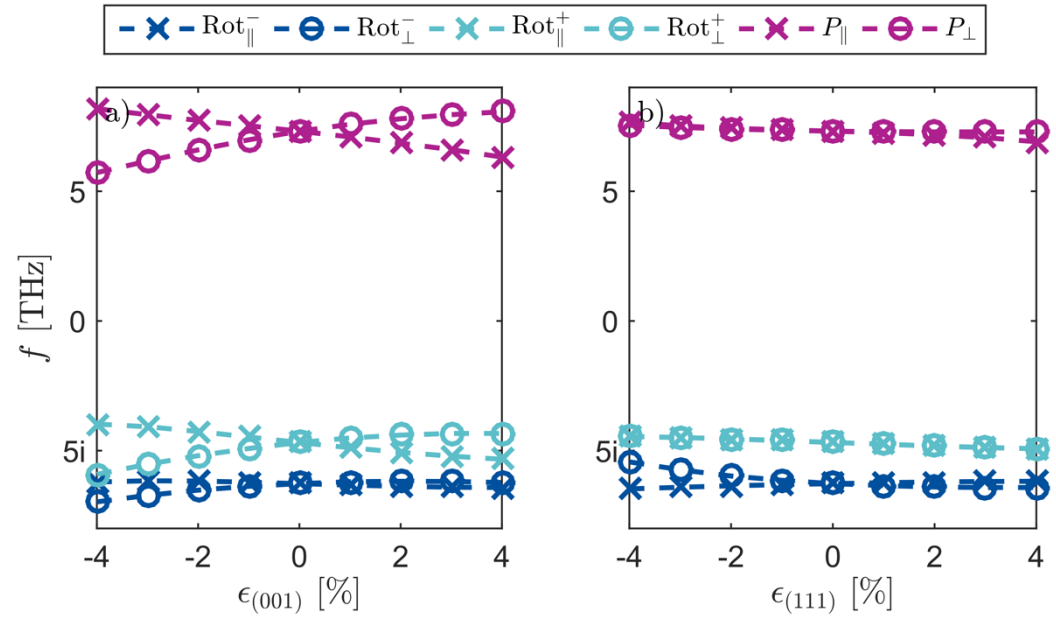

Figure S5: the frequencies of the three different phonon modes considered as a function of in-plane strain in the a) (001)-plane and b) (111)-plane for $LaFeO_3$.

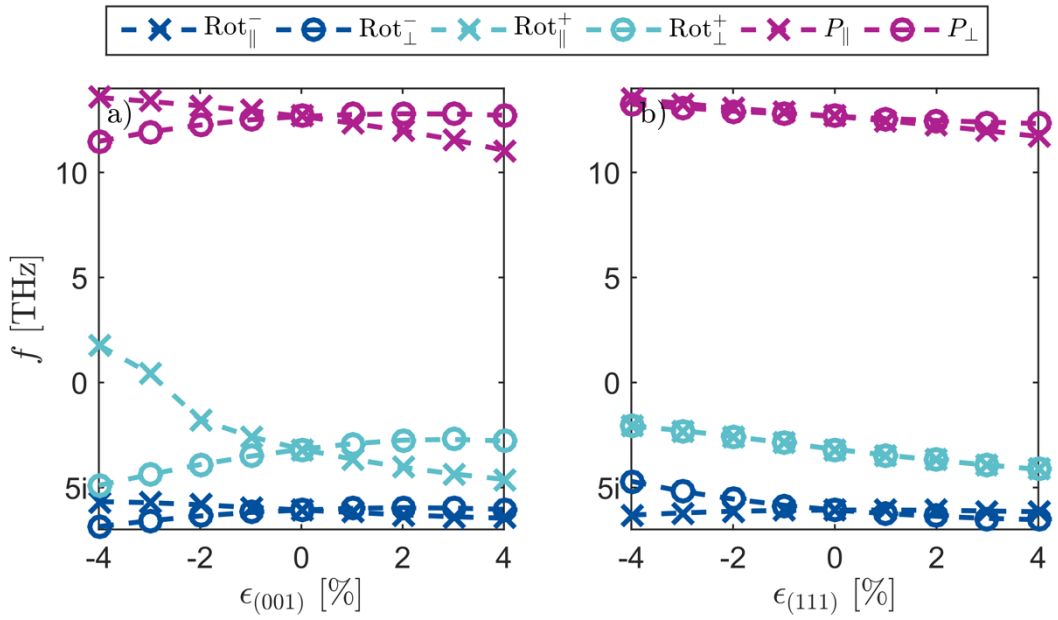

Figure S6: the frequencies of the three different phonon modes considered as a function of in-plane strain in the a) (001)-plane and b) (111)-plane for $NdGaO_3$.

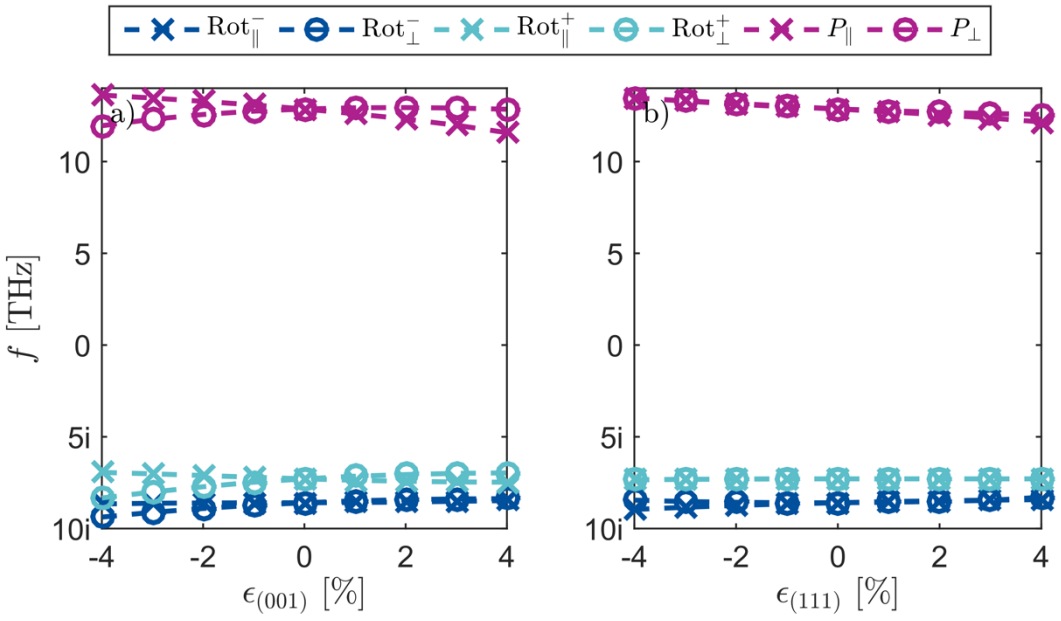

Figure S7: the frequencies of the three different phonon modes considered as a function of in-plane strain in the a) (001)-plane and b) (111)-plane for $YAlO_3$.

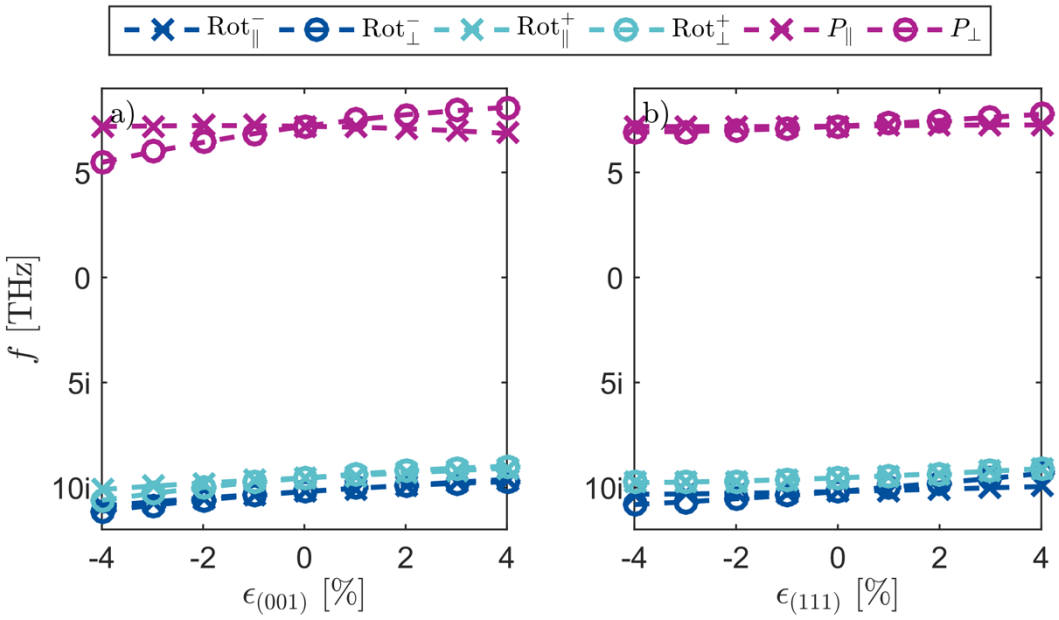

Figure S8: the frequencies of the three different phonon modes considered as a function of in-plane strain in the a) (001)-plane and b) (111)-plane for $GdScO_3$.

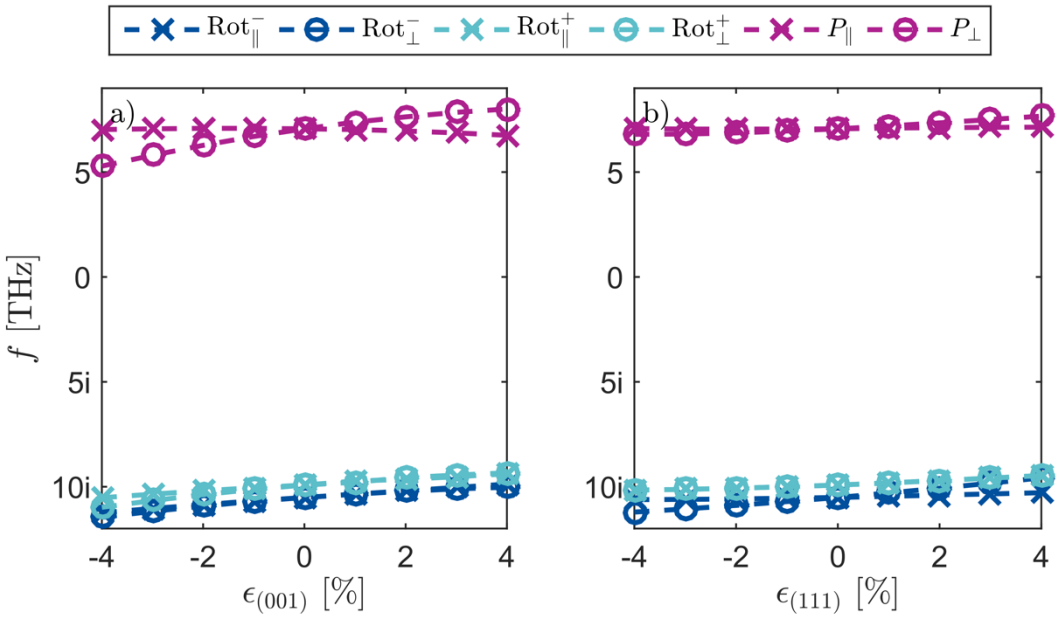

Figure S9: the frequencies of the three different phonon modes considered as a function of in-plane strain in the a) (001)-plane and b) (111)-plane for $DyScO_3$.

II-IV Perovskites

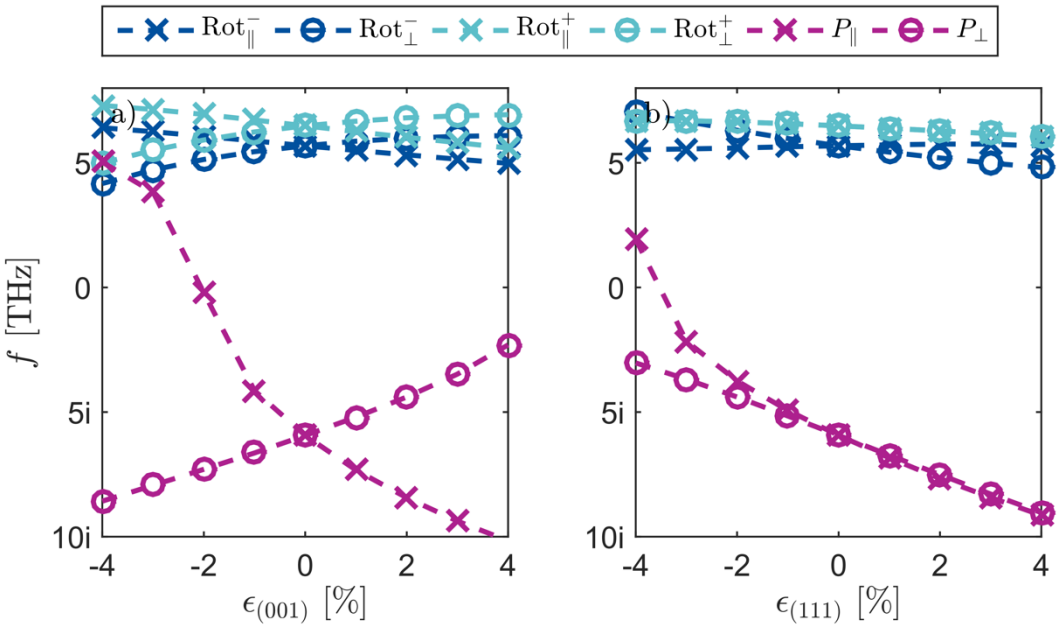

Figure S10: the frequencies of the three different phonon modes considered as a function of in-plane strain in the a) (001)-plane and b) (111)-plane for $BaTiO_3$.

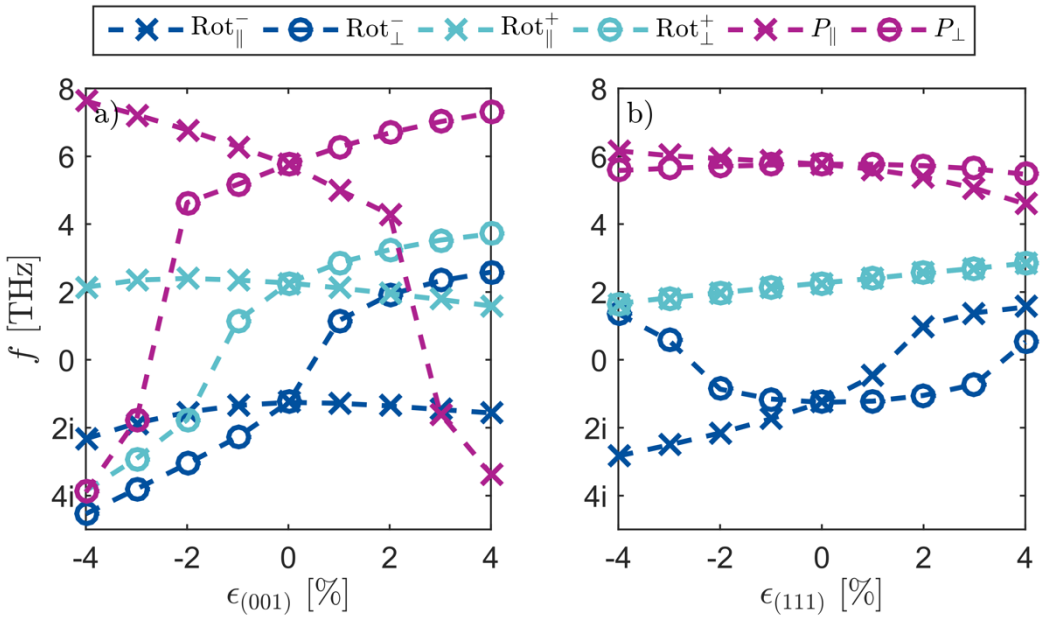

Figure S11: the frequencies of the three different phonon modes considered as a function of in-plane strain in the a) (001)-plane and b) (111)-plane for $BaZrO_3$.

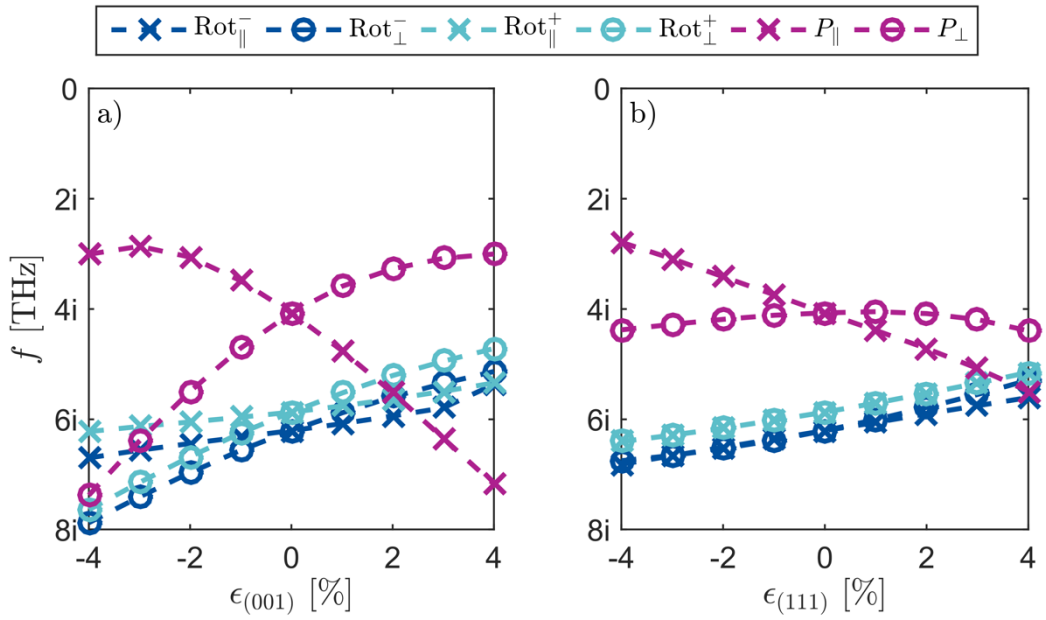

Figure S12: the frequencies of the three different phonon modes considered as a function of in-plane strain in the a) (001)-plane and b) (111)-plane for $CaTiO_3$.

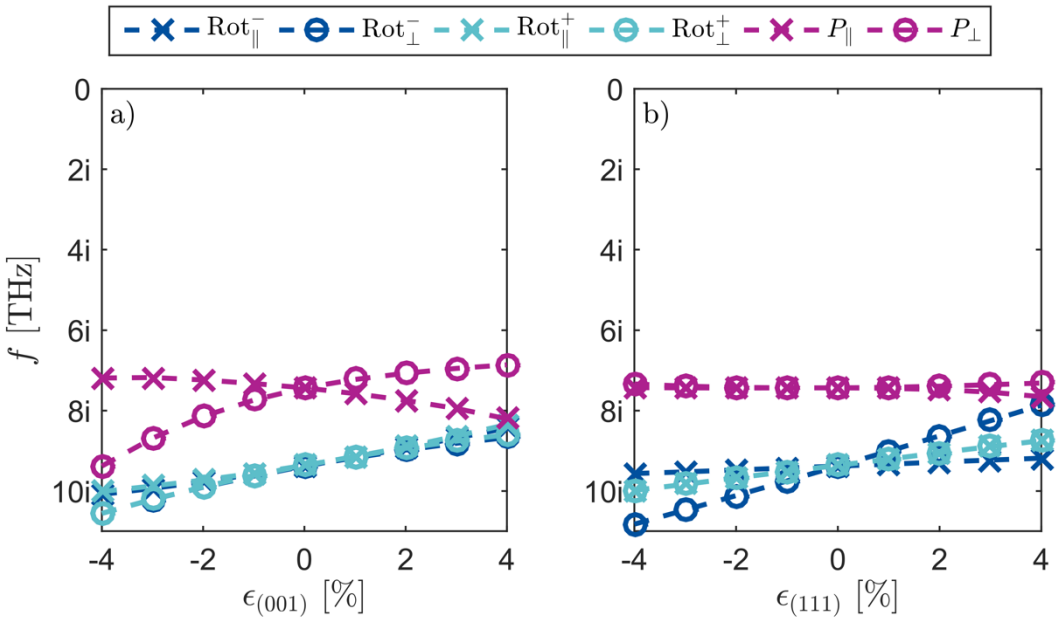

Figure S13: the frequencies of the three different phonon modes considered as a function of in-plane strain in the a) (001)-plane and b) (111)-plane for $SrZrO_3$.

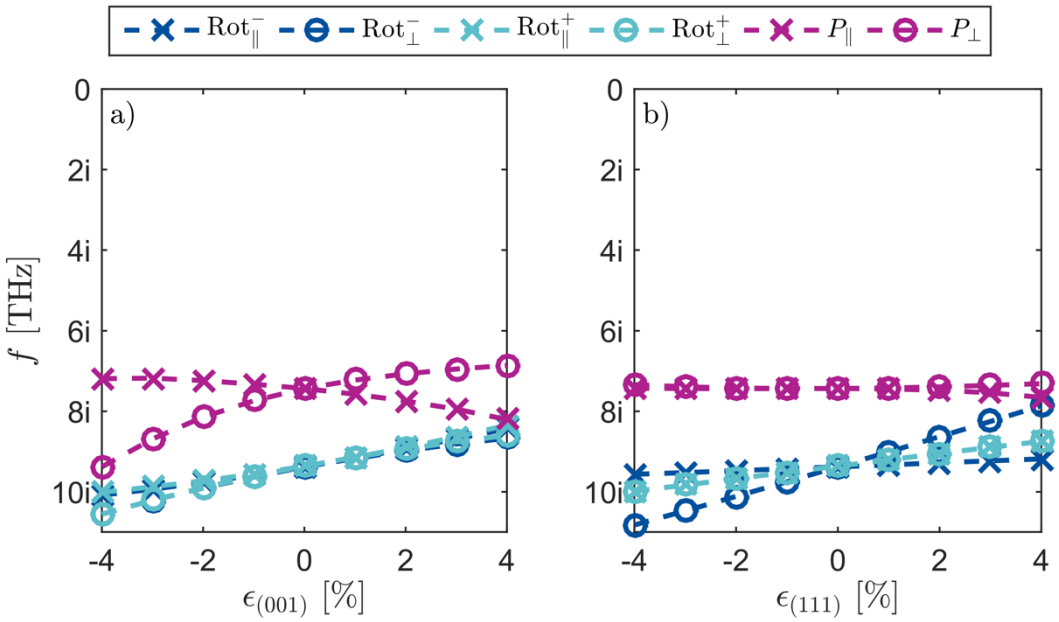

Figure S14: the frequencies of the three different phonon modes considered as a function of in-plane strain in the a) (001)-plane and b) (111)-plane for $MgTiO_3$.

I-V Perovskites

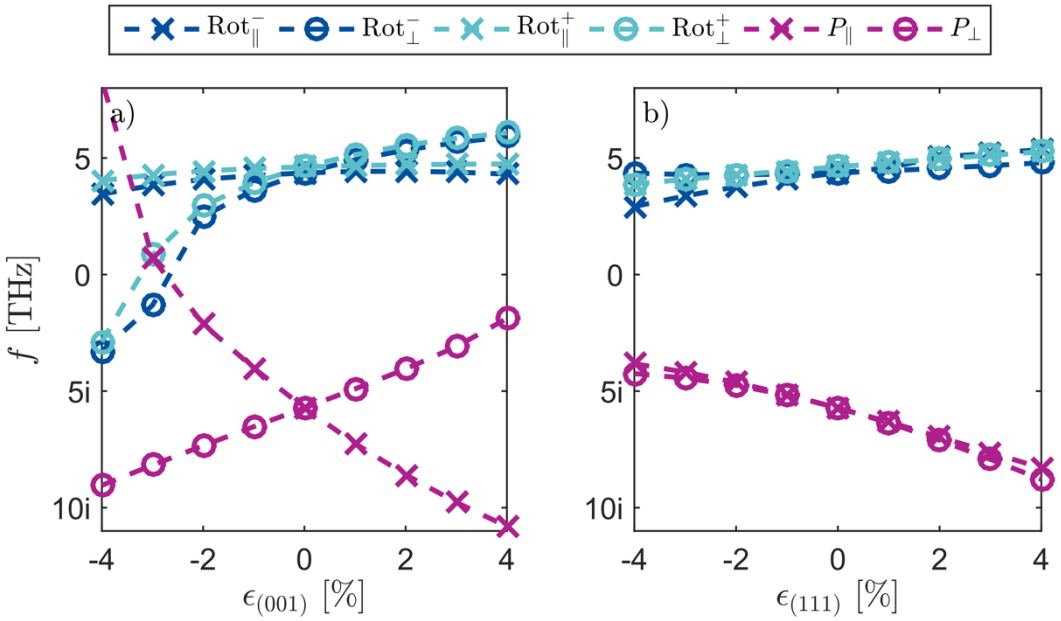

Figure S15: the frequencies of the three different phonon modes considered as a function of in-plane strain in the a) (001)-plane and b) (111)-plane for $KNbO_3$.

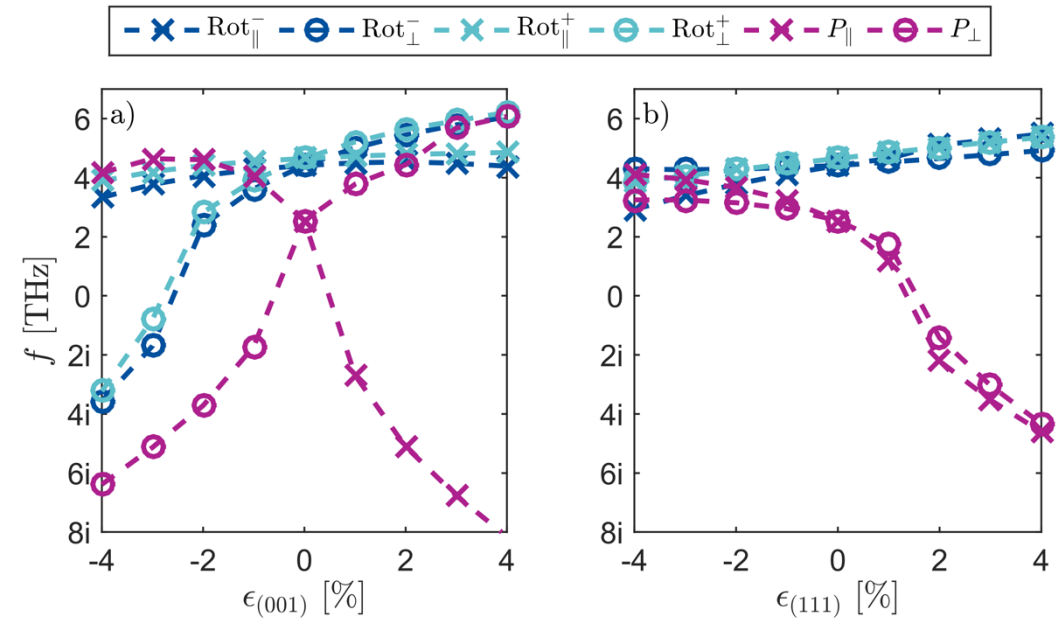

Figure S16: the frequencies of the three different phonon modes considered as a function of in-plane strain in the a) (001)-plane and b) (111)-plane for $KTaO_3$.

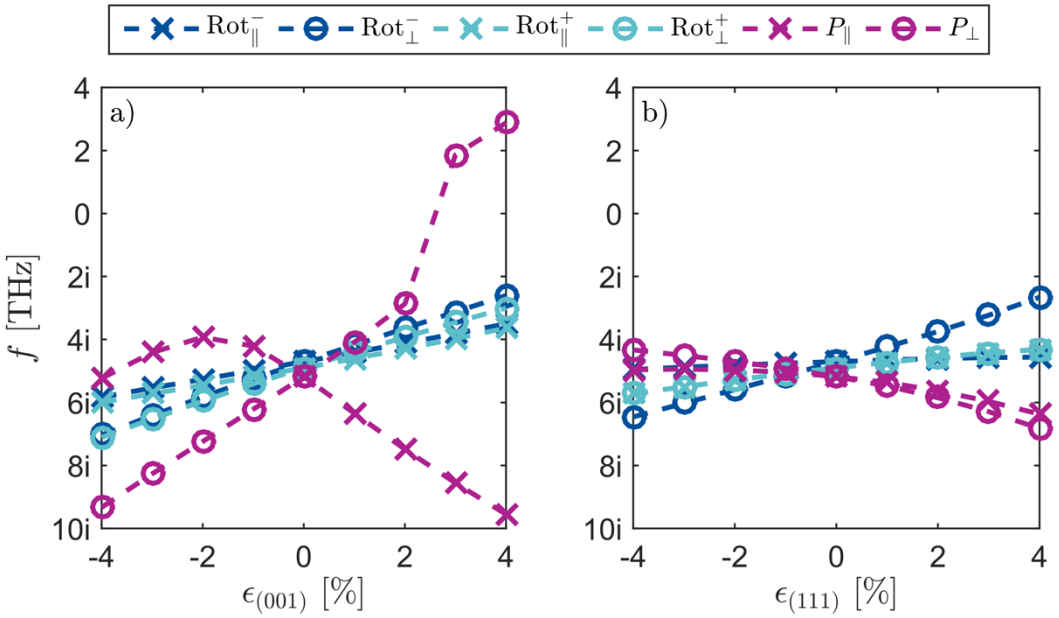

Figure S17: the frequencies of the three different phonon modes considered as a function of in-plane strain in the a) (001)-plane and b) (111)-plane for $AgNbO_3$.

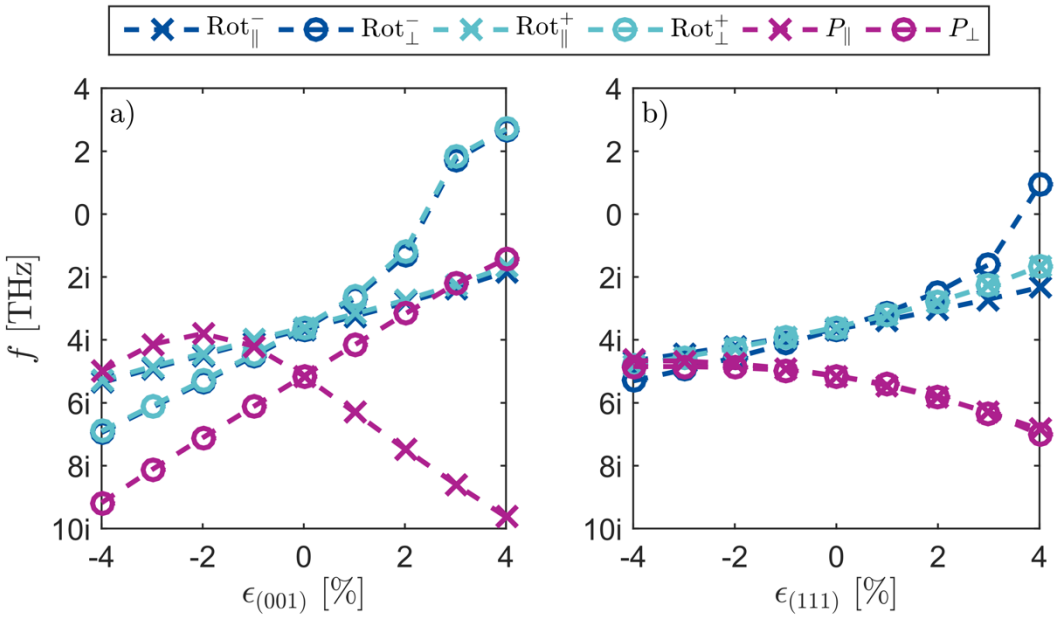

Figure S18: the frequencies of the three different phonon modes considered as a function of in-plane strain in the a) (001)-plane and b) (111)-plane for $NaNbO_3$.

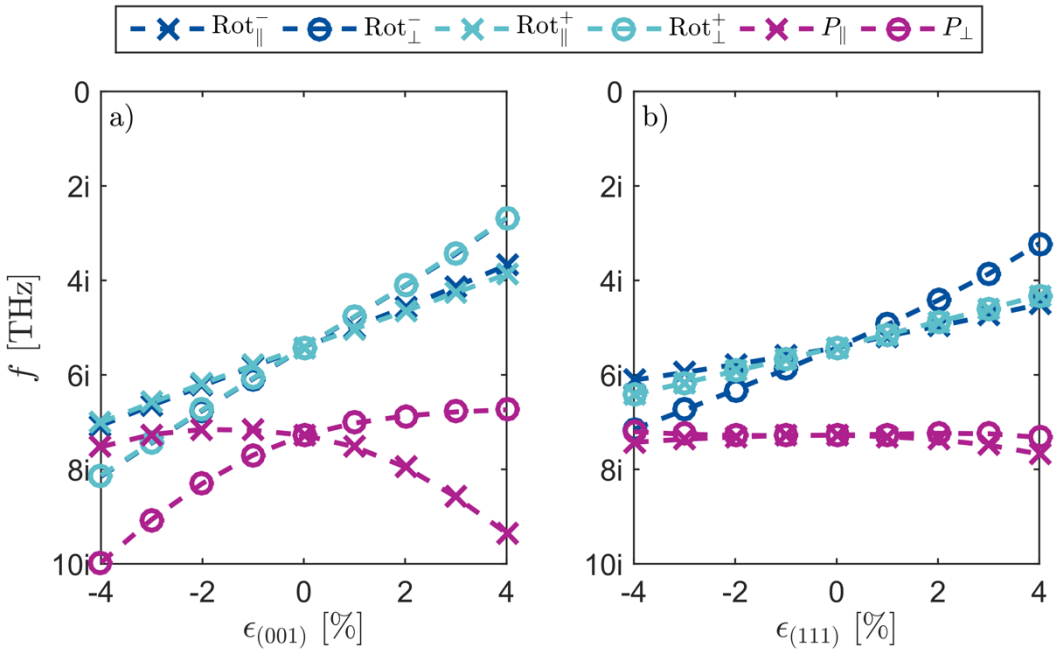

Figure S19: the frequencies of the three different phonon modes considered as a function of in-plane strain in the a) (001)-plane and b) (111)-plane for $LiNbO_3$.

CONTRIBUTIONS OF A- AND B-CATIONS TO POLAR MODE

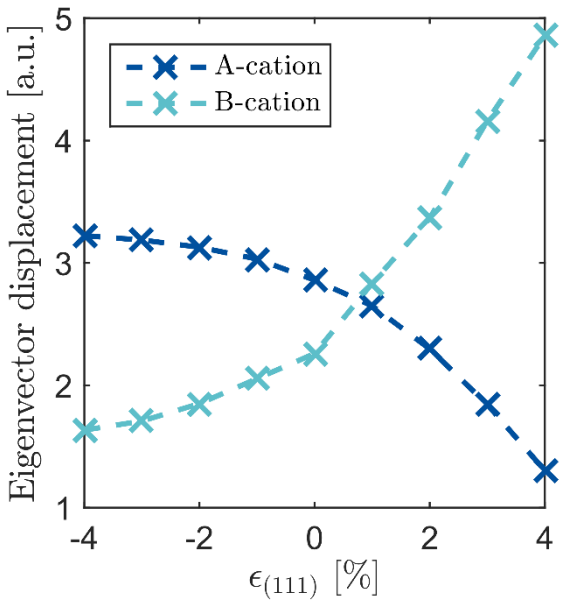

Figure S20: the displacement relative displacements of the A- and B-cation of $NaTaO_3$ under (111)-strain for the out-of-plane polar mode, given by the relative eigenvector amplitude times the atomic mass. As seen, there is a crossover from A-cation dominated to B-cation dominated at 1 % compressive strain e.g. right before the point where the $df_{pol,\perp}/d\epsilon_{(111)}$ changes sign as shown in Figure 4 b in the main manuscript.

IN-PLANE POLAR MODES

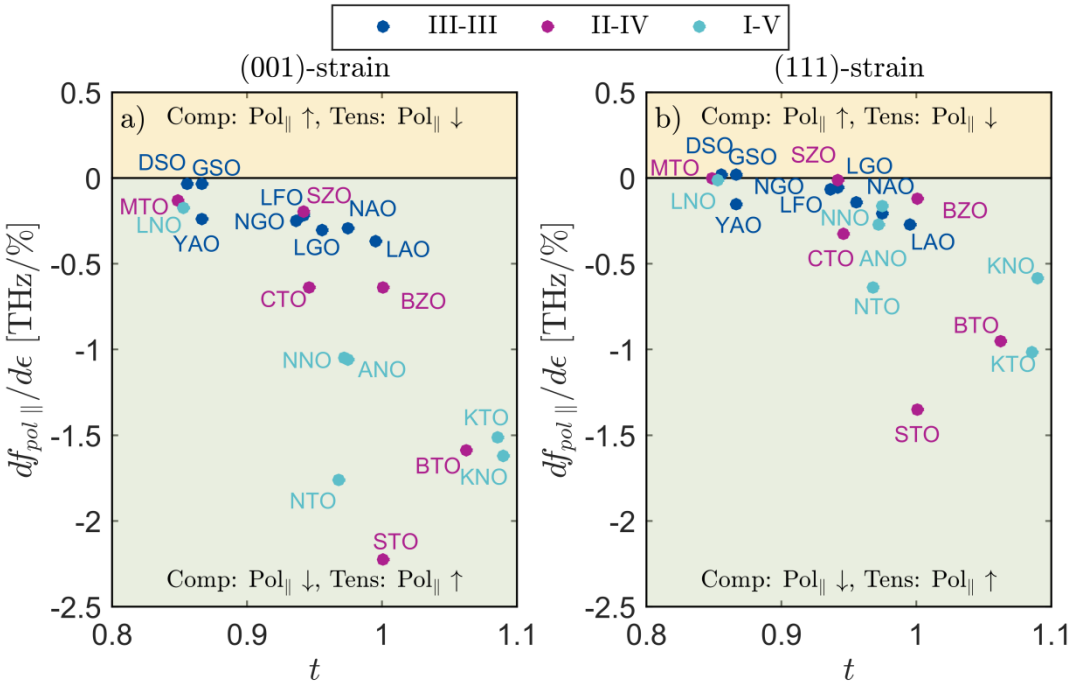

Figure S21: Derivative of the out-of-plane polar modes as a function of tolerance factor t with respect to a) (001)-strain and b) (111)-strain as a function of tolerance factor t. A positive $df/d\epsilon$, yellow area, means that the respective mode is softened by compressive (comp) strain and hardened by tensile (tens) strain, while a negative $df/d\epsilon$, green area, means that the respective mode is softened by tens strain and hardened for comp strain and favored for tens strain. See Table I in the main manuscript for abbreviations. The in-plane polar modes show similar behavior for both (001)- and (111)-strain.